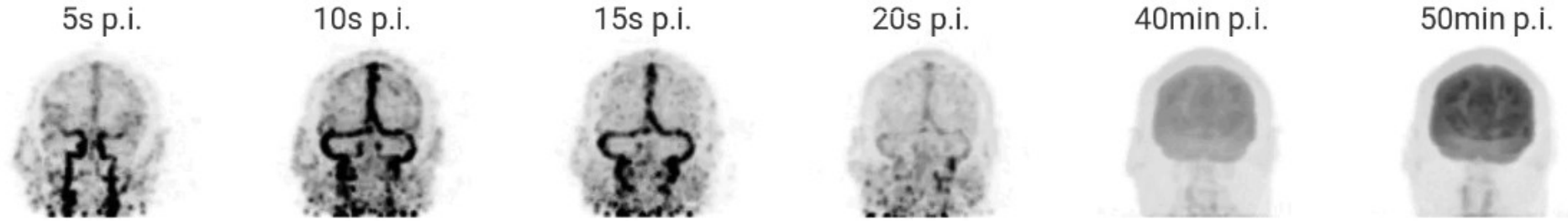


# **Review of selected PET image correction approaches using machine learning methods**

Michał Obara

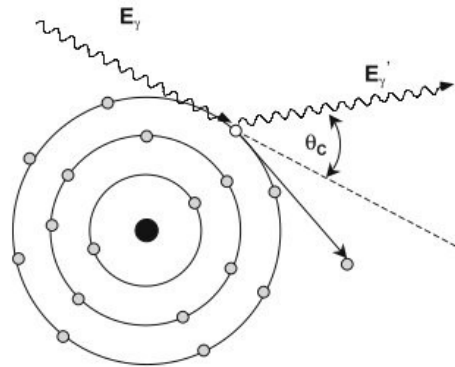
13.01.2025

# PET events detection

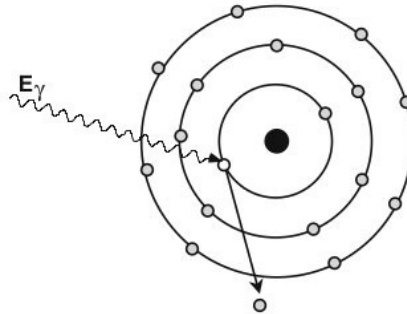


18F-FDG distribution in time

Georg Schramm, KU Leuven

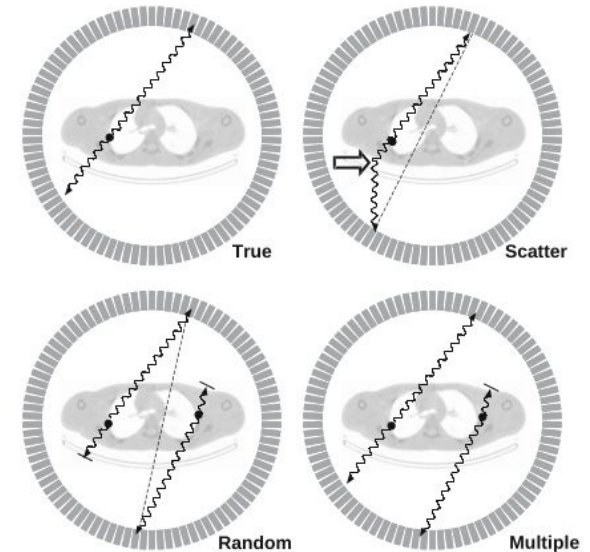


Compton scattering



Photoelectric effect

Dale L Bailey, PET Basic Sciences



Coincidence events types

# Scatter corrections

## Single Scatter Simulation:

- Monte Carlo simulation of single scattered photons
- Using attenuation map and an initial activity estimation
- Does not directly consider multiple scattering
- Standard method in clinical PET
- Computational complexity

## Machine learning techniques:

- End-to-end U-Net
  - Low-quality PET → high-quality PET
  - Uncorrected PET + CT → corrected PET
  - CT → PET or AC PET → CT

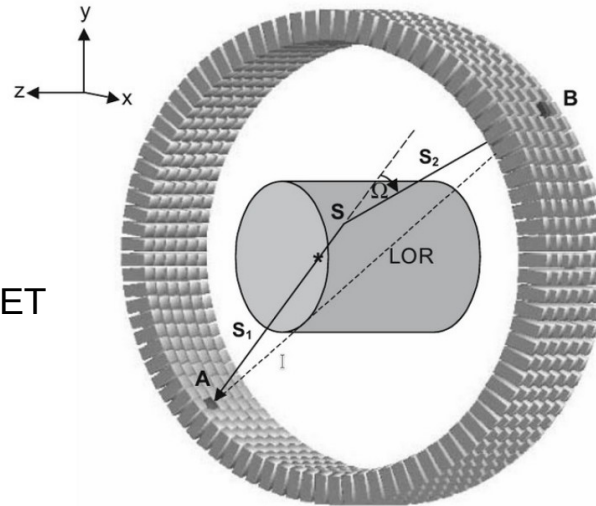
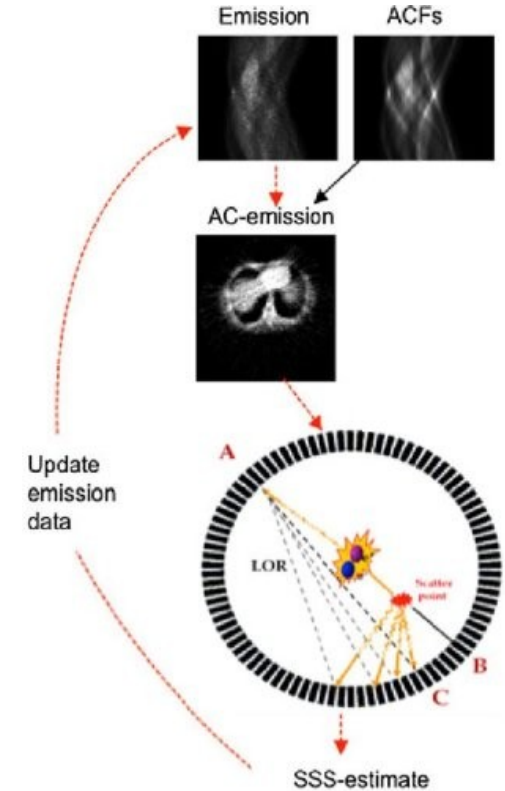


Figure 5.16. Geometry of the single scattering model used in simulation based scatter correction.

Dale L Bailey, PET Basic Sciences



DOI 10.1007/s12149-011-0514-y

# Huang et al., 2023

<https://doi.org/10.1007/s00259-023-06422-x>

Comment > [Eur J Nucl Med Mol Imaging](#). 2023 Dec;51(1):27-39.

doi: [10.1007/s00259-023-06422-x](https://doi.org/10.1007/s00259-023-06422-x). Epub 2023 Sep 6.

## Short-axis PET image quality improvement based on a uEXPLORER total-body PET system through deep learning

Zhenxing Huang <sup># 1</sup>, Wenbo Li <sup># 1</sup>, Yaping Wu <sup># 2</sup>, Nannan Guo <sup>1 3</sup>, Lin Yang <sup>1 3</sup>, Na Zhang <sup>1</sup>, Zhifeng Pang <sup>3</sup>, Yongfeng Yang <sup>1</sup>, Yun Zhou <sup>4</sup>, Yue Shang <sup>5</sup>, Hairong Zheng <sup>1</sup>, Dong Liang <sup>1</sup>, Meiyun Wang <sup>6</sup>, Zhanli Hu <sup>7</sup>

Affiliations + expand

PMID: 37672046 DOI: [10.1007/s00259-023-06422-x](https://doi.org/10.1007/s00259-023-06422-x)

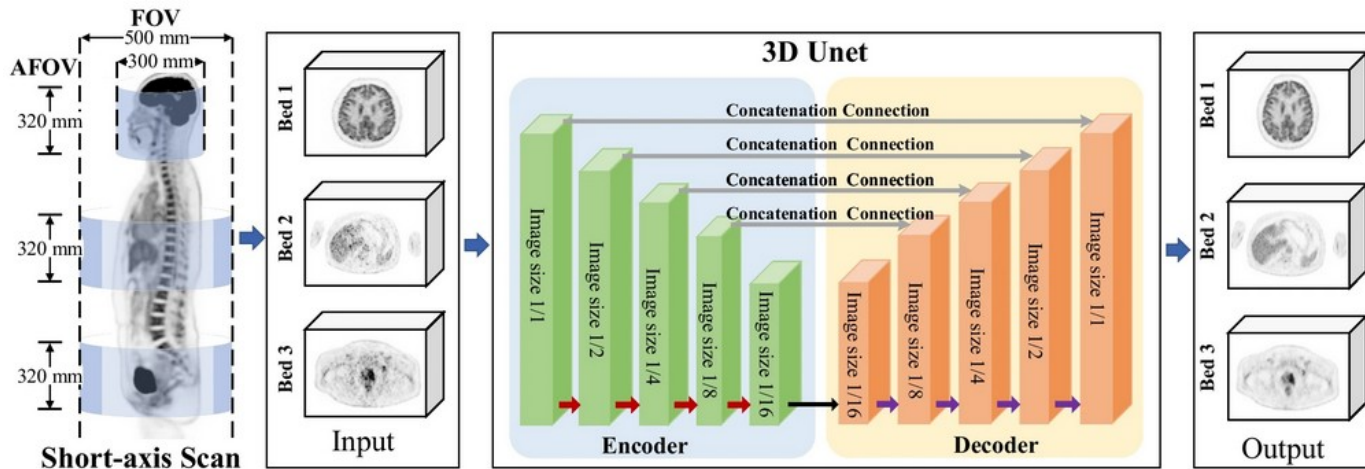
# Huang et al., 2023

## Data:

- uEXPLORER PET/CT images from 335 patients (18F-FDG)
- Two sets of PET images:
  - High-Quality PET (HQ-PET): Total-body PET images (1940 mm AFOV)
  - Low-Quality PET (LQ-PET): Simulated short-axis PET images (320–500 mm AFOV)

## Model:

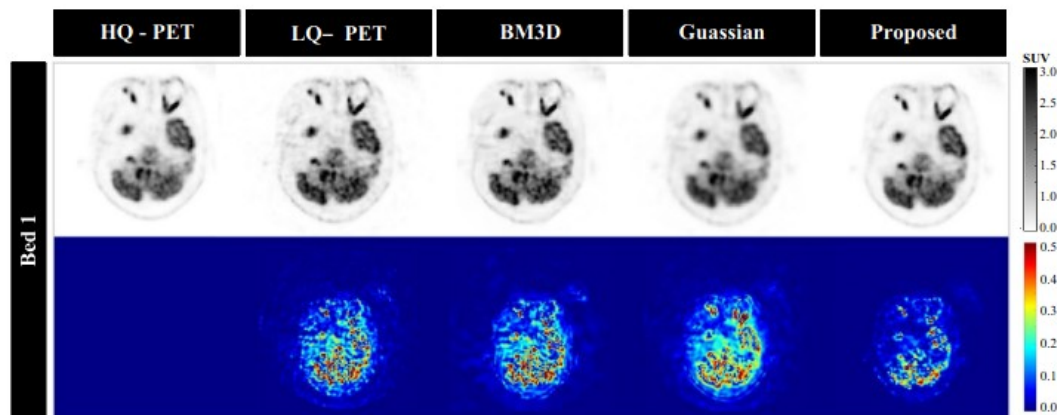
- A 3D U-Net trained to map LQ-PET to HQ-PET images
- Separate training for brain, lung, and abdomen datasets
- Split: 300/35, loss: MAE, batch size: 16, Optimizer: Adam, epochs: 500



# Huang et al., 2023

## Evaluation Metrics:

- Quantitative: Peak Signal-to-Noise Ratio (PSNR) and Structural Similarity Index Measure (SSIM) comparison to HQ-PET and traditional denoising methods
- Qualitative: clinical evaluation by nuclear medicine experts using a 5-point scoring system



## Results:

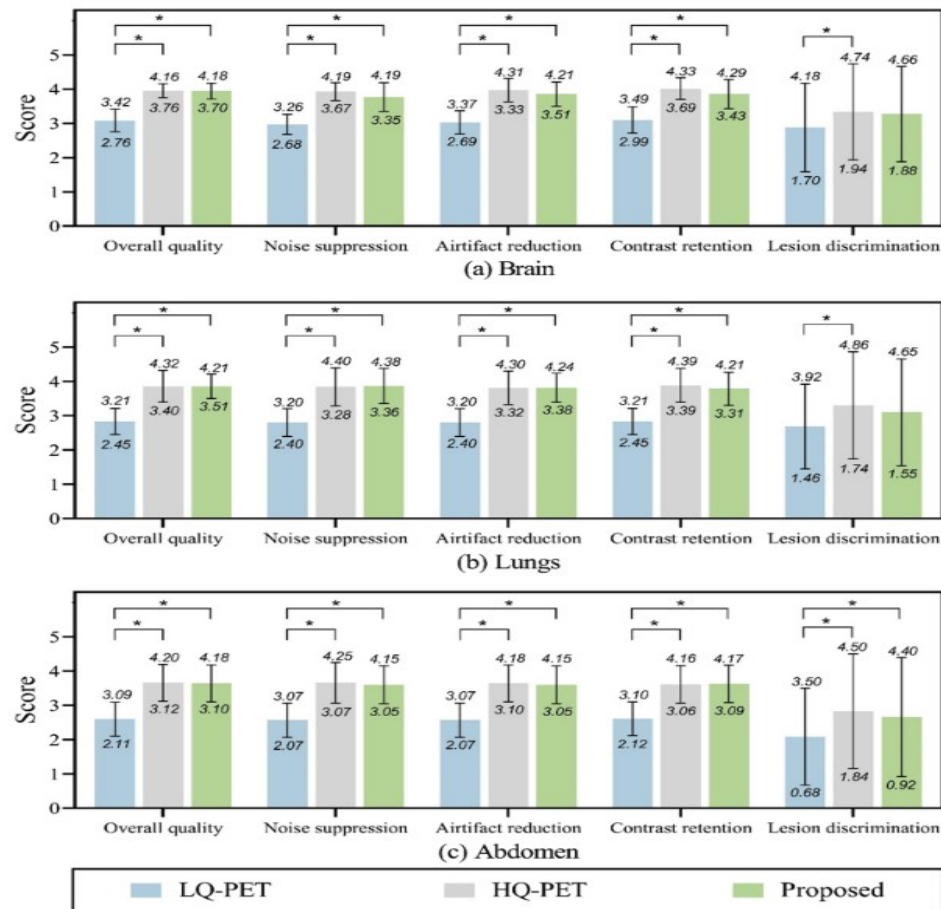
- Quantitative evaluation:

Beds	LQ-PET		Gaussian		BM3D		Proposed	
	PSNR	SSIM	PSNR	SSIM	PSNR	SSIM	PSNR	SSIM
Bed 1	$34.54 \pm 5.14$	$0.91 \pm 0.09$	$28.66 \pm 3.3^*$	$0.86 \pm 0.10^*$	$30.88 \pm 6.38^*$	$0.51 \pm 0.24^*$	$35.41 \pm 5.45^*$	$0.94 \pm 0.15^*$
Bed 2	$32.16 \pm 6.22$	$0.92 \pm 0.04$	$30.95 \pm 3.68^*$	$0.91 \pm 0.05^*$	$29.45 \pm 5.49^*$	$0.41 \pm 0.17^*$	$33.77 \pm 6.18^*$	$0.95 \pm 0.03^*$
Bed 3	$36.65 \pm 6.97$	$0.94 \pm 0.04$	$30.76 \pm 4.57^*$	$0.91 \pm 0.05^*$	$30.55 \pm 8.47^*$	$0.43 \pm 0.27^*$	$38.58 \pm 7.28^*$	$0.97 \pm 0.03^*$

# Huang et al., 2023

## Results:

- Qualitative Evaluation:
  - Proposed method significantly improved scores across all categories vs. LQ-PET
  - Overall quality for Proposed is close to HQ-PET, far exceeding LQ-PET





## Physics in Medicine & Biology



### PAPER

# PET scatter estimation using deep learning U-Net architecture

**RECEIVED**

13 June 2022

**REVISED**



15 September 2022

**ACCEPTED FOR PUBLICATION**

13 October 2022

**PUBLISHED**

10 March 2023

Baptiste Laurent<sup>1,\*</sup> , Alexandre Bousse<sup>1</sup> , Thibaut Merlin<sup>1</sup>, Stephan Nekolla<sup>2</sup> and Dimitris Visvikis<sup>1</sup>

<sup>1</sup> LaTIM, INSERM, UMR 1101, UBO, Brest, France

<sup>2</sup> Department of Nuclear Medicine, Klinikum rechts der Isar der Technischen Universität München, Munich, Germany

\* Author to whom any correspondence should be addressed.

**E-mail:** [baptiste.laurent@univ-brest.fr](mailto:baptiste.laurent@univ-brest.fr)

**Keywords:** PET, reconstruction, scatter estimation, scatter correction, deep learning



# Laurent et al., 2023

## Data:

- GATE simulations with XCAT phantoms.
- Variations in anatomy (lung, pelvis regions) and body morphologies (S, M, L)
- 216 simulated datasets with acquisition durations of 1–6 minutes
- Two clinical Biograph mMR images

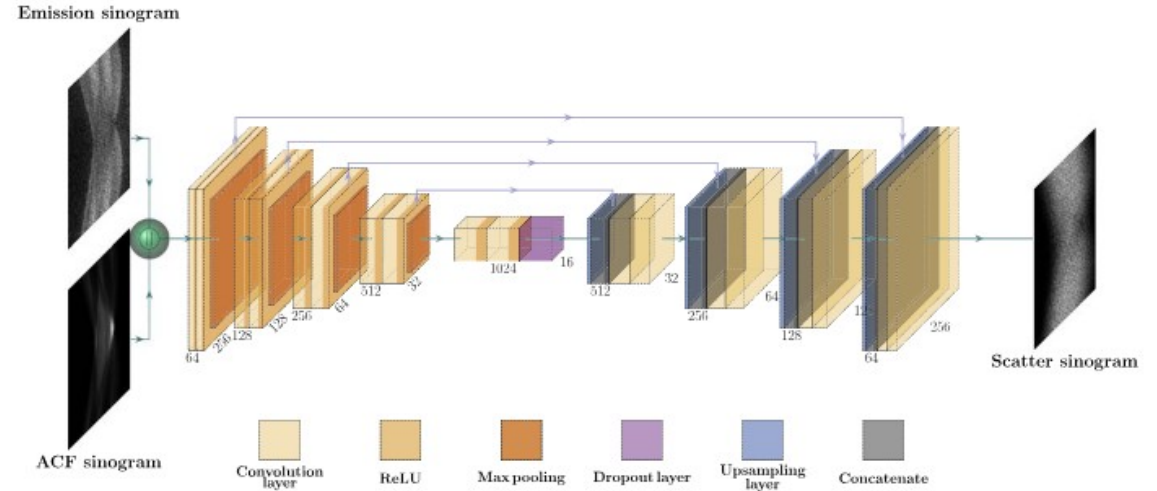
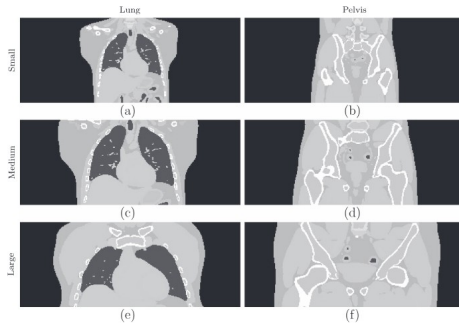


**Figure 1.** DLSE architecture, based on a CNN U-Net architecture. The network takes emission and attenuation sinograms as input, to predict scatter sinogram.

## Model:

- U-Net architecture
- Input: PET emission and attenuation factor (AF) sinograms.  
output: estimated scatter sinogram
- Loss: MSE, batch size: 8, epochs: 100

	Small	Medium	Large
Total body height (mm)	1227	1752	2103
Chest short axis (AP) (mm)	163	232	279
Chest Long axis (LAT) (mm)	228	325	391
Chest circumference (mm)	696	993	1194
Waist short axis (AP) (mm)	163	233	335
Waist long axis (LAT) (mm)	202	288	416

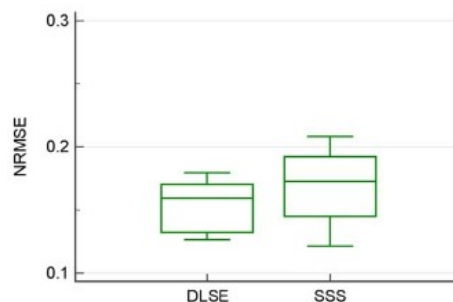
# Laurent et al., 2023

## Evaluation:

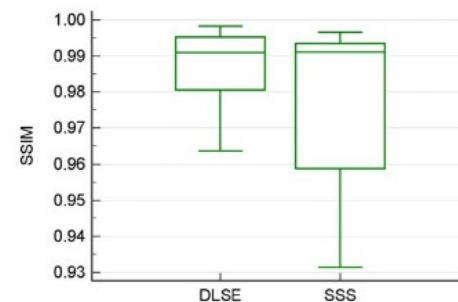
- Metrics: Normalized Root Mean Square Error (NRMSE) and Structural Similarity Index (SSIM)
- Comparison with SSS and ground truth
- Tested on reconstructed PET images with simulated lesions and two clinical datasets

## Results:

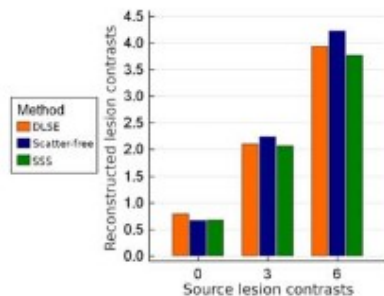
- DLSE achieves lower NRMSE and higher SSIM than SSS
- Better contrast recovery for hot lesions (3:1 and 6:1) than SSS
- Slight overestimation in cold lesions (0:1)



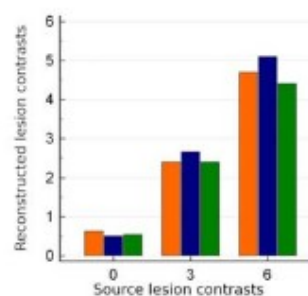
(a) NRMSE



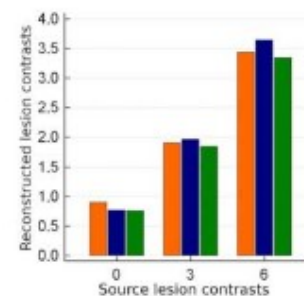
(b) SSIM



(a) Contrasts for lesions of all ROIs



(b) Contrasts for lesions in liver



(c) Contrast for lesions in lungs

# Ben-Cohen et al., 2019

<https://doi.org/10.1016/j.engappai.2018.11.013>





## Engineering Applications of Artificial Intelligence

Volume 78, February 2019, Pages 186-194



### Cross-modality synthesis from CT to PET using FCN and GAN networks for improved automated lesion detection ☆

Avi Ben-Cohen<sup>a</sup>  , Eyal Klang<sup>b</sup>, Stephen P. Raskin<sup>b</sup>, Shelly Soffer<sup>b</sup>, Simona Ben-Haim<sup>c,d</sup>,  
Eli Konen<sup>b</sup>, Michal Marianne Amitai<sup>b,1</sup>, Hayit Greenspan<sup>a,1</sup>

# Ben-Cohen et al., 2019

## Objective:

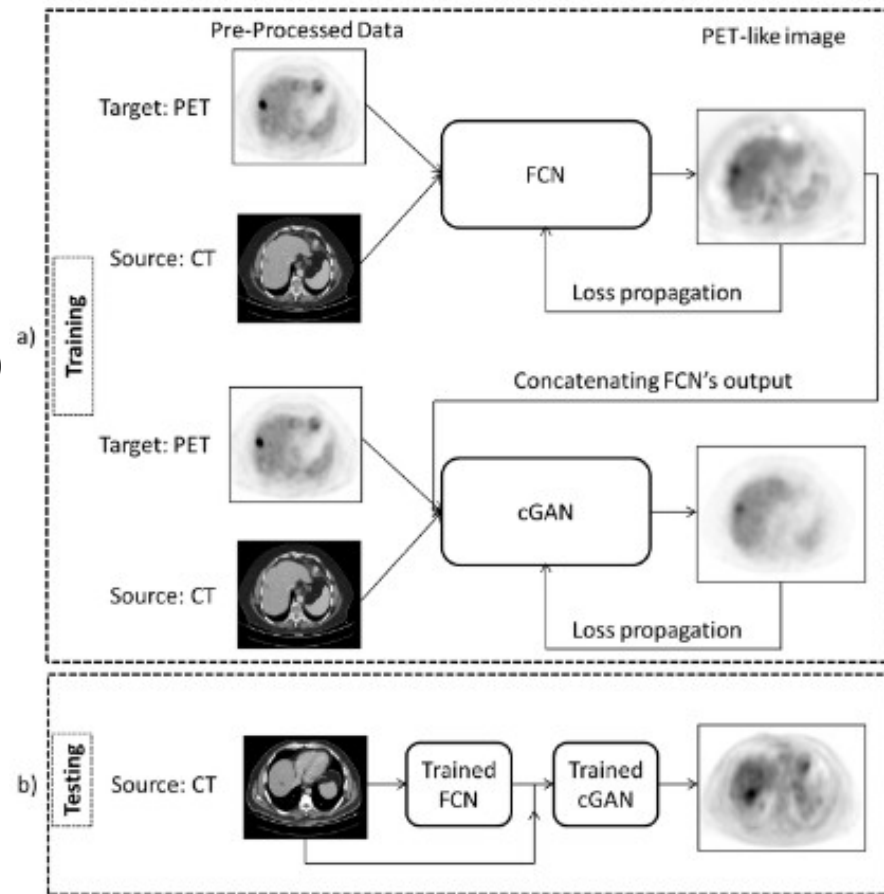
- Generate PET/CT from CT scans
- Reduce PET/CT cost and radiation
- Improve liver lesion detection

## Dataset:

- 60 PET/CT clinical scans
- Training: 23 pairs (6 malignant); testing: 37 pairs (9 malignant)
- Focused on liver region.

## Model:

- FCN (VGG-16 based) generates initial PET-like images from CT data, loss: L2, optimizer: Adam,
- cGAN (conditional GAN) refines outputs using U-Net generator and a custom L2 loss function
- Augmentation: scaling, translation, random noise



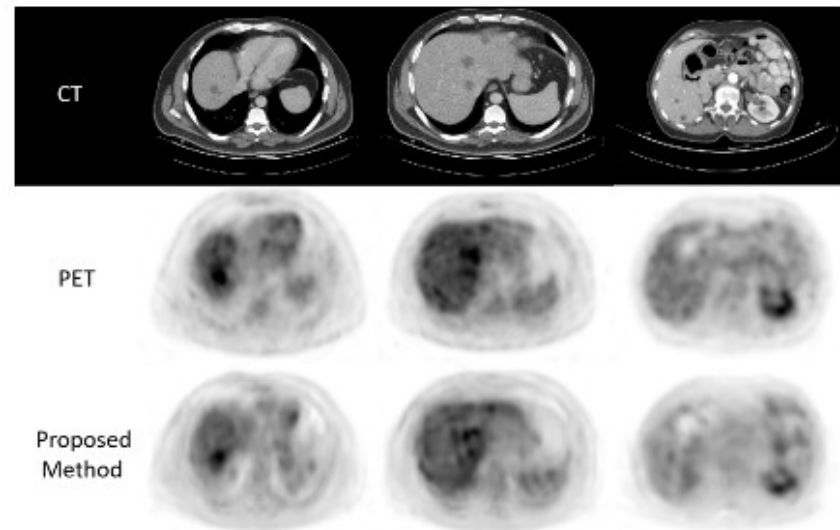
# Ben-Cohen et al., 2019

## Evaluation:

- Reconstruction metrics:
  - PSNR (overall reconstruction quality)
  - MAE – calculated for high (> 2.5) and low (<2.5) SUV sep.
- Detection performance:
- Tested on liver lesion detection system
- Metrics: TPR, FPS

## Results:

- Reconstruction results:
  - High SUV gives lower results



	Method	High SUV		Low SUV		Average Score	
		MAE	PSNR	MAE	PSNR	MAE	PSNR
Combined	*FCN-4s-cGAN Eq. (8)	<b>1.33 ± 0.65</b>	22.40 ± 2.92	0.11 ± 0.04	38.04 ± 1.92	<b>0.72 ± 0.35</b>	30.22 ± 2.42
	*FCN-4s-cGAN Eq. (7)	1.48 ± 0.66	21.70 ± 2.95	<b>0.09 ± 0.05</b>	<b>39.1 ± 1.95</b>	0.79 ± 0.36	<b>30.4 ± 2.45</b>
	FCN-4s-cGAN L2	1.55 ± 0.66	21.10 ± 2.94	0.10 ± 0.04	39.03 ± 1.94	0.83 ± 0.35	30.07 ± 2.44
	Blending	1.50 ± 0.63	21.40 ± 2.94	0.10 ± 0.04	39.00 ± 2.03	0.80 ± 0.34	30.20 ± 2.49
cGAN	cGAN-U-Net gen.	1.70 ± 0.61	20.62 ± 2.92	0.10 ± 0.04	39.06 ± 1.90	0.90 ± 0.33	29.84 ± 2.41
	cGAN-FCN-4s gen.	1.52 ± 0.63	21.10 ± 3.10	0.12 ± 0.04	37.60 ± 1.95	0.82 ± 0.34	29.35 ± 2.53
FCN	FCN-4s	<b>1.33 ± 0.59</b>	<b>22.50 ± 2.93</b>	0.16 ± 0.05	37.60 ± 1.99	0.74 ± 0.32	30.05 ± 2.46
	FCN-8s	<b>1.33 ± 0.57</b>	22.45 ± 2.92	0.15 ± 0.05	37.63 ± 1.99	0.74 ± 0.31	30.04 ± 2.46
	FCN-2s	1.37 ± 0.62	22.42 ± 3.02	0.14 ± 0.05	37.70 ± 2.02	0.76 ± 0.34	30.06 ± 2.52
	U-Net	1.52 ± 0.67	21.57 ± 3.1	0.12 ± 0.04	38.56 ± 1.74	0.82 ± 0.36	30.07 ± 2.42

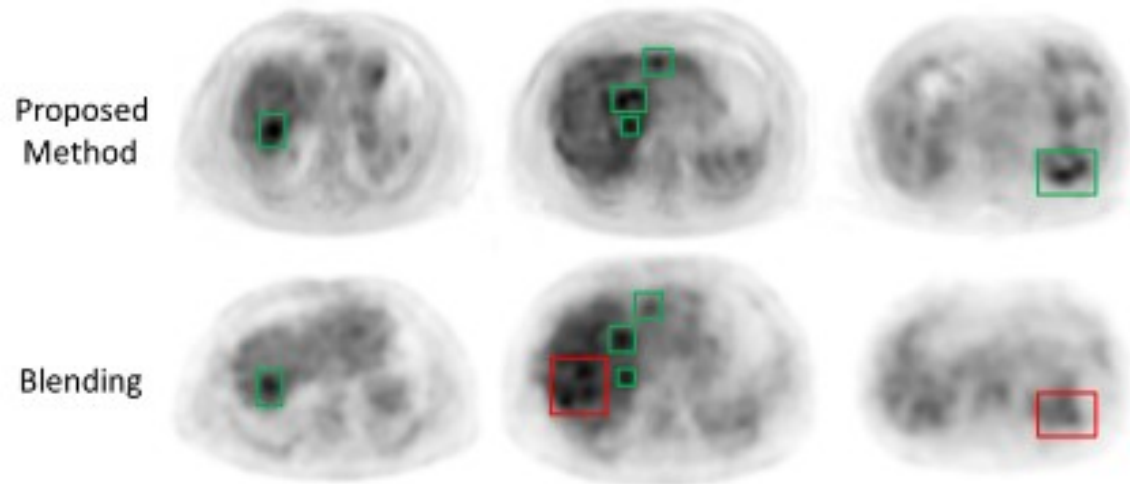
\*Proposed method

# Ben-Cohen et al., 2019

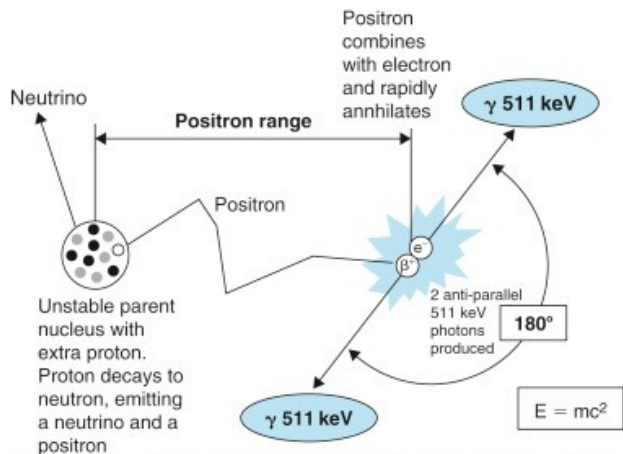
## Results:

- Detection results:
  - Maintained high TPR (96.4%)
  - Decreased FPR (2.9% to 2.1%)
  - No comparison to regular PET

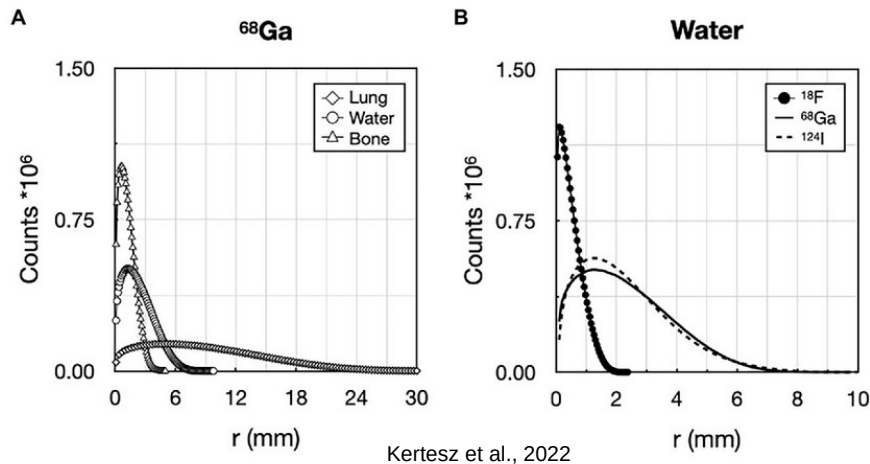
Method	TPR[%]	Average FPR
Detection soft.	94.6	2.9 ± 2.1
Detection soft+ proposed	<b>94.6</b>	<b>2.1 ± 1.7</b>
Detection soft+ blending	90.9	2.2 ± 1.7
Detection soft+ FCN-4s	90.9	2.2 ± 1.7



# Positron range



Marie Foley Kijewski, in Handbook of Neuro-Oncology Neuroimaging



Nuclide	$E_{\max}$ (MeV)	$E_{\text{mode}}$ (MeV)	$t_{1/2}$ (mins)	Range in Water (mm)		Use in PET
				Max	Mean	
$^{11}\text{C}$	0.959	0.326	20.4	4.1	1.1	Labelling of organic molecules
$^{13}\text{N}$	1.197	0.432	9.96	5.1	1.5	$^{13}\text{NH}_3$
$^{15}\text{O}$	1.738	0.696	2.03	7.3	2.5	$^{15}\text{O}_2$ , $\text{H}_2^{15}\text{O}$ , $\text{C}^{15}\text{O}$ , $\text{C}^{15}\text{O}_2$
$^{18}\text{F}$	0.633	0.202	109.8	2.4	0.6	$^{18}\text{F}$ -DG, $^{18}\text{F}$ -
$^{68}\text{Ga}$	1.898	0.783	68.3	8.2	2.9	$^{68}\text{Ga}$ -EDTA, $^{68}\text{Ga}$ -PTSM
$^{82}\text{Rb}$	3.40	1.385	1.25	14.1	5.9	Generator-produced perfusion tracer
$^{94\text{m}}\text{Tc}$	2.44	†	52	‡	‡	$\beta^+$ -emitting version of $^{99\text{m}}\text{Tc}$
$^{124}\text{I}$	2.13	†	$6.0 \times 10^3$	‡	‡	Iodinated molecules

†Not reported to date.  
‡Many-positron decay scheme hence no  $E_{\text{mode}}$  value given.

Dale L Bailey, PET Basic Sciences



# Herraiz et al., 2020

<https://doi.org/10.3390/app11010266>

## Deep-Learning Based Positron Range Correction of PET Images

by Joaquín L. Herrera<sup>1,2,\*</sup>  , Adrián Bembibre<sup>1</sup>   and Alejandro López-Montes<sup>1</sup>  

<sup>1</sup> Nuclear Physics Group and IPARCOS, Faculty of Physical Sciences, University Complutense of Madrid, CEI Moncloa, 28040 Madrid, Spain

<sup>2</sup> Health Research Institute of the Hospital Clínico San Carlos (IdISSC), 28040 Madrid, Spain

\* Author to whom correspondence should be addressed.

*Appl. Sci.* **2021**, *11*(1), 266; <https://doi.org/10.3390/app11010266>

**Submission received: 28 November 2020 / Revised: 21 December 2020 / Accepted: 25 December 2020 /**

**Published: 29 December 2020**

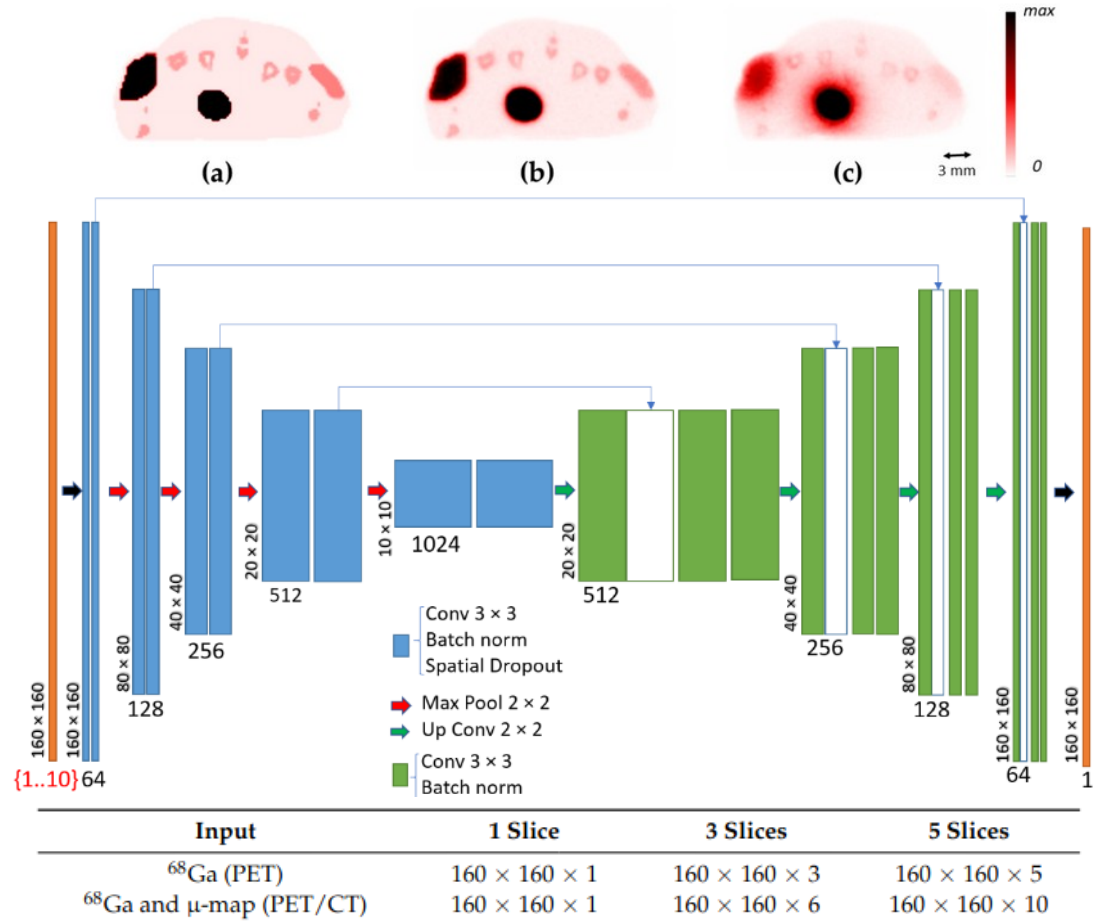
# Herraiz et al., 2020

## Data:

- 8 Simulated PET mice images for  $^{18}\text{F}$  and  $^{68}\text{Ga}$
- Voxel size: 0.28 mm
- Augmented with flips, shifts, and rotations

## Model:

- U-Net architecture
- Input:  $^{68}\text{Ga}$  PET images (with or without  $\mu$ -maps)
- Output: PR-corrected images matching  $^{18}\text{F}$  reference images.
- Optimizer: Rectified Adam, loss: L1, epochs: 50



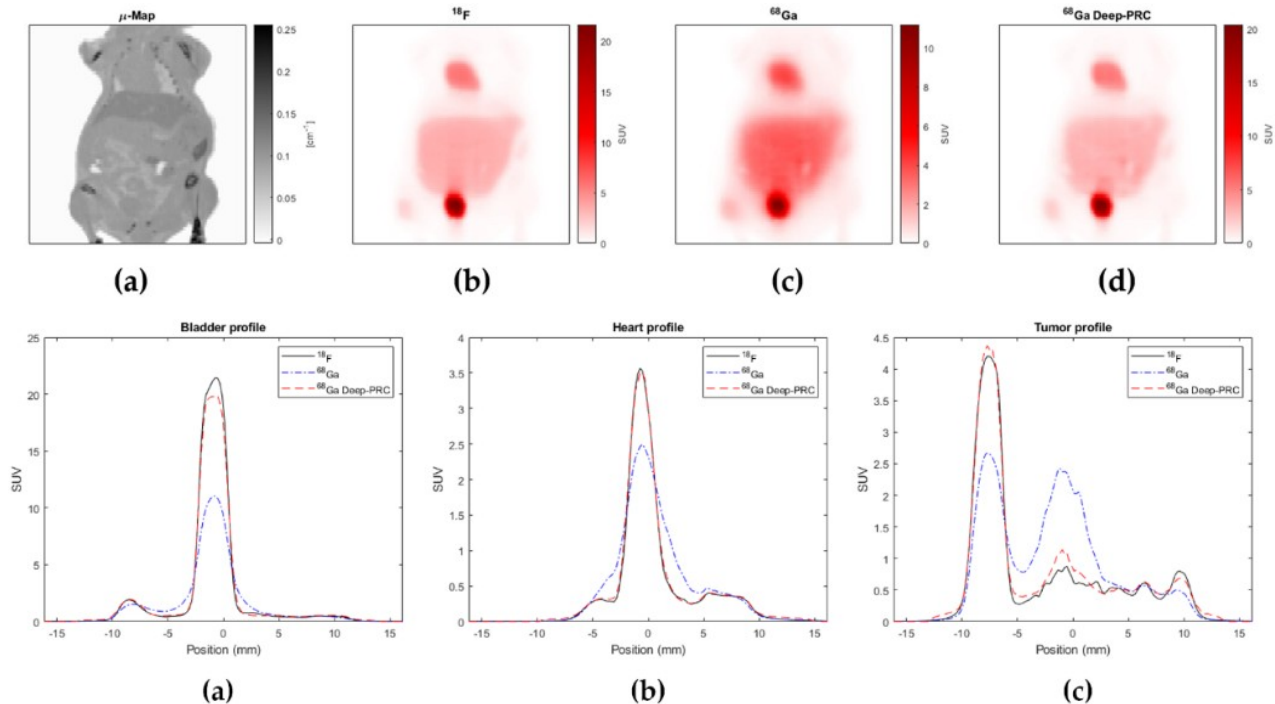
# Herraiz et al., 2020

## Evaluation:

- Comparison:  $^{68}\text{Ga}$  PET before and after correction vs.  $^{18}\text{F}$  reference.
- Metrics: Recovery (%) / "defining regions over the whole organ" / and noise ( $\sigma/\mu$ ).
- Test data: Simulated PET not in training/validation.

## Results:

- Recovery: >95% match to  $^{18}\text{F}$  images.
- Noise: Comparable to reference  $^{18}\text{F}$  PET.
- Input: PET-only sufficient for accurate correction.



	Recovery (%)			Noise (%)		
	Heart	Bladder	Tumor	Heart	Bladder	Tumor
$^{18}\text{F}$	100.00	100.00	100.00	2.00	3.75	3.39
$^{68}\text{Ga}$	67.41	53.49	60.50	4.03	4.96	4.08
$^{68}\text{Ga}$ Deep-PRC	95.19	96.16	97.46	2.52	3.96	3.02

# Shiri et al., 2022

<https://doi.org/10.1007/s00259-022-06053-8>

## Federated Learning

- What? Collaborative model training without data sharing
- Why? Ensuring data privacy and leveraging multicenter datasets

*European Journal of Nuclear Medicine and Molecular Imaging* • Open Access • Volume 50, Issue 4, Pages 1034 - 1050 • March 2023

## Decentralized collaborative multi-institutional PET attenuation and scatter correction using federated deep learning

[Shiri, Isaac<sup>a</sup>](#); [Vafaei Sadr, Alireza<sup>b, c</sup>](#); [Akhavan, Azadeh<sup>a</sup>](#);  
[Salimi, Yazdan<sup>a</sup>](#); [Sanaat, Amirhossein<sup>a</sup>](#); [Amini, Mehdi<sup>a</sup>](#);  
[Razeghi, Behrooz<sup>d</sup>](#); [Saber, Abdollah<sup>a</sup>](#); [Arabi, Hossein<sup>a</sup>](#);  
[Ferdowsi, Sohrab<sup>e</sup>](#); [Voloshynovskiy, Slava<sup>d</sup>](#); [Gündüz, Deniz<sup>f</sup>](#)

[Show additional authors](#)   Save all to author list

28 97th percentile  
Citations in Scopus

6.05  
FWCI 

3  
Views count 

[View all metrics](#) 

# Shiri et al., 2022

## Dataset:

- 6 centers, 50 pairs of 18F-FDG PET (NAC + CT ASC) images each
- Standardized PET images to SUV units with uniform voxel size ( $3 \times 3 \times 4$  mm<sup>3</sup>)
- Normalized intensities to a consistent range (0 to 5) across all centers

**Table 1** Patients demographics and PET/CT image acquisition and reconstruction settings across the six different centers

		Centre 1	Centre 2	Centre 3	Centre 4	Centre 5	Centre 6
Demographic	Sex (F/M)	15/35	17/33	19/31	22/28	6/44	21/29
	Age	$54 \pm 22.7$	$62.6 \pm 8.8$	$63.9 \pm 12.2$	$68 \pm 9.4$	$58.2 \pm 9$	$52.6 \pm 20.2$
	Weight	$69.1 \pm 15.9$	$68.2 \pm 18.4$	$77.3 \pm 18.7$	$74.5 \pm 16.1$	$84.3 \pm 18$	$70.2 \pm 23.3$
Scanners	Manufacture	GE	GE	GE	GE	GE	Siemens
	Model	Duo	LS	ST	Discovery 690	RX	Biograph
CT acquisition	Average tube current	$115.7 \pm 9.2$	$120.6 \pm 41$	$149.2 \pm 51.9$	$98.3 \pm 61$	$264.1 \pm 41.9$	$176 \pm 32.0$
	kVp	$130 \pm 0$	$135 \pm 8.8$	$134 \pm 9.3$	$134 \pm 9.3$	$119.2 \pm 4$	$130 \pm 0$
PET acquisition and reconstruction parameters	Injected dose	$487.2 \pm 72.9$	$514.3 \pm 118.1$	$549.7 \pm 95.2$	$425.5 \pm 91.2$	$448.9 \pm 121.8$	$373.9 \pm 92.6$
	Time to scan	$75.7 \pm 18.9$	$72.1 \pm 25.5$	$75.2 \pm 17.6$	$73.1 \pm 18.8$	$86.7 \pm 13.6$	$97.6 \pm 13.9$
	Time Per Bed	$2.6 \pm 0.5$	$4.6 \pm 1$	$3.6 \pm 0.6$	$2.4 \pm 1$	$3.1 \pm 0.3$	$3.1 \pm 0.4$
	Scatter Correction	Model-based	Convolution subtraction	Convolution subtraction	Model-based	Model-based	Model-based
	Reconstruction	OSEM	OSEM	OSEM	VPHD, VPHDS	OSEM	OSEM+PSF
	Matrix size	$256 \times 256$	$128 \times 128$	$128 \times 128$	$192 \times 192$	$128 \times 128$	$168 \times 168$
	Slice thickness	3.4	4.3	3.3	3.5	3.3	3
	Slice numbers	14,598	10,647	13,683	16,282	11,002	26,210

# Shiri et al., 2022

## Model:

- Architecture: Modified U2-Net with residual blocks
- Input: Non-AC/SC PET images
- Output: AC/SC-corrected PET images
- Training: Adam optimizer, L2 loss, learning rate 0.001

## Methodology:

- **FL Sequential (FL-SQ)**

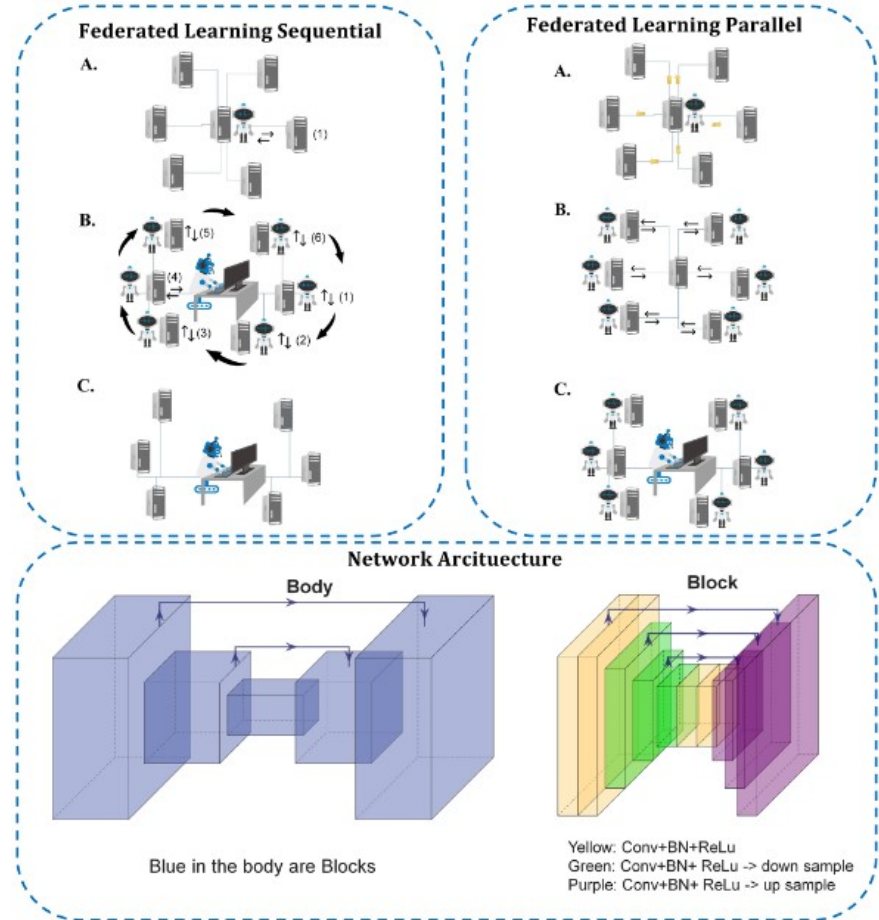
- A) model meets data center-after-center
- B) model passes sequentially through all centers
- C) process repeats for number of rounds

- **FL Parallel (FL-PL)**

- A) models are trained separately in each node
- B) central model is distributed across all nodes
- C) local models are returned to central server and aggregate to central global model

- **Centralized (CZ)**

- **Center based (CB)**





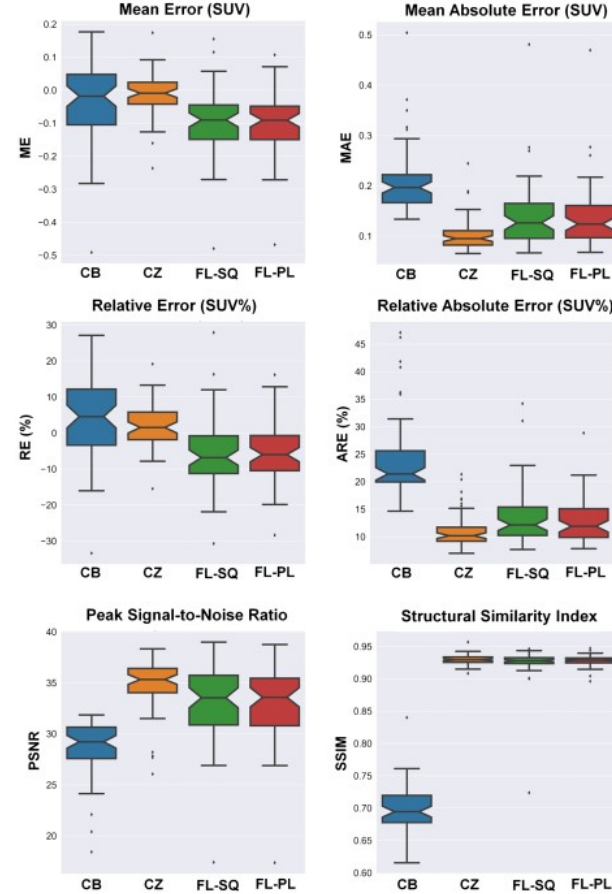
# Shiri et al., 2022

## Evaluation & results:

- Metrics: AE, MAE, RE, RAE, PSNR, SSIM
- FL (PL, SQ): comparable to CZ, significantly better than CB
- CB: Poor generalization due to isolated data

## Limitations:

- Simulated setup; real-world use may face communication and computational challenges
- FL models are sensitive to noise and artifacts, requiring monitoring





Thank you :)